59th ILMENAU SCIENTIFIC COLLOQUIUM
Technische Universität Ilmenau, 11 – 15 September 2017
URN: urn:nbn:de:gbv:ilm1-2017iwk-104:5

OPTIMIZATION OF THE OPTICAL PARAMETERS IN FABRY-PEROT INTERFEROMETER

Yung-Cheng Wang[1], Lih-Horng Shyu[2], Pi-Cheng Tung[3], Hung-Ta Shih[3], Jui-Cheng Lin[4], Bean-Yin Lee[5], Jhe-Sian Li [1]

[1] Department of Mechanical Engineering, National Yunlin University of Science and Technology
[2] Department of Electro-Optical Engineering, National Formosa University
[3] Department of Mechanical Engineering, National Central University
[4] Department of Mechanical Design Engineering, National Formosa University
[5] Department of Mechanical and computer-Aided Engineering, National Formosa University

ABSTRACT

Due to insensitivity to the environmental disturbances, Fabry-Perot interferometers are suitable for displacement measurements under ordinary conditions. In the structure of folded Fabry-Perot interferometer, the results of the signal subdivision are affected by the optical parameters in the resonant cavity. In this paper, the analysis of the Fabry-Perot interferometer for the measurement of the micro-displacement and the long-distance are investigated. By considering the reflectance of the planar mirror and the intensity loss in the resonant cavity, the parameters of systematic optimization which are suitable for the measurement of the micro-displacement and the long-distance are proposed. The experimental and simulated results reveal that the intensity loss in the resonant cavity is 86% and the optimized reflectance of the planar mirror is 12%.

Keyword - Fabry-Perot interferometer, Displacement measurement, Resonant cavity.

1. INTRODUCTION

Commercial interferometers are with the structure of the non-common optical path, hence the reference beam and the measurement beam are traveling in the different directions. Although the Michelson interferometer has the advantages of simple signal processing, it is sensitive to the environmental disturbances relatively. In view of the above, the Fabry-Perot interferometer of the common optical path is constructed to realize the high resistance to the environmental disturbances.

To simplify the signal processing of the Fabry-Perot interferometer, the optical elements are necessary to be arranged to the resonant cavity and the reflectance of the planar mirror has to be adjusted to change the interferometric signal. However, the complicated resonant cavity and the planar mirror of the different reflectance will lead to more intensity loss and the change of the interferometric finesse. Therefore, according to the previous study which is focused on the folded Fabry-Perot interferometer, a simulation analysis by considering the intensity loss and the reflectance of the planar mirror to achieve the purpose of optimization of the optical parameters in this study.

2. THEORETICAL FORMULAS

The optical structure can be applied to the different measurement objective as shown in Fig. 1. Laser beam passes through the BS into the optical cavity. The one-eighth waveplate in the

©2017 - TU Ilmenau

cavity is utilized to form the orthogonal phase shift between interferometric signals. The polarization axis of the waveplate must be the same as that of PBS. By this arrangement, the orthogonal signal can be acquired by two photodiodes (PDs) and then transmitted to the signal processing module.

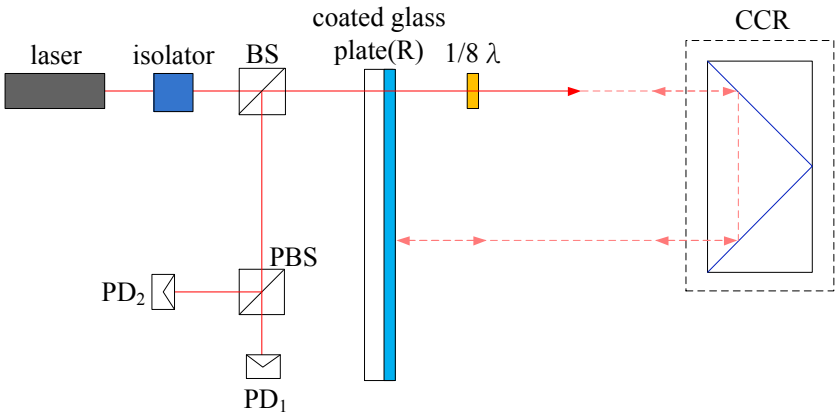

Fig. 1 Optical structure of the interferometer

The corresponding equation of the folded Fabry-Perot interferometer can be derived as followings. The amplitude of the firstly reflected beam is expressed as A_{S1} (2.1) and other interferometric beams can be denoted with A_{Sn} (2.2), where A_0 is the amplitude of incident light wave, R is the reflectance of the coated glass plate, L is the resultant transmittance of the optical cavity, and n is the order number of the backward reflected light beam.

$$A_{S1} = \frac{-1}{2\sqrt{2}} A_0 \sqrt{R} \tag{2.1}$$

$$A_{Sn} = \frac{1}{2\sqrt{2}} A_0 T(L)^{n-1} (\sqrt{R})^{2n-3} \tag{2.2}$$

The corresponding electric field of the interferometric beam can be described as Eq. 2.3 and 2.4, where δ is the phase difference of the optical path. In this structure, δ is $\frac{4\pi d}{\lambda}$, d is the distance between the planar mirror and CCR, ω is the angular frequency.

$$E_{Sn} = \frac{1}{2\sqrt{2}} A_0 T(L)^{n-1} (\sqrt{R})^{2n-3} e^{i(\omega t - kx + (2n-2)\cdot\delta)} \tag{2.3}$$

$$E_{Pn} = \frac{1}{2\sqrt{2}} A_0 T(L)^{n-1} (\sqrt{R})^{2n-3} e^{i(\omega t - kx + (2n-2)\cdot\delta - \frac{\pi}{2})} \tag{2.4}$$

By Eq. 2.5 and 2.6, the intensity distribution of s-type and p-type can be denoted with Eq. 2.7

and Eq. 2.8.

$$I_S = E_s \cdot E_s^* \tag{2.5}$$

$$I_P = E_p \cdot E_p^* \tag{2.6}$$

For s-type (PD1) intensity,

$$I_S = E_s \cdot E_s^* = \frac{1}{8} A_0^2 \frac{R(1+L^2)-2LR\cos(2\delta)}{1+L^2R^2-2LR\cos(2\delta)} \tag{2.7}$$

For p-type (PD2) intensity,

$$I_P = E_p \cdot E_p^* = \frac{1}{8} A_0^2 \frac{R(1+L^2)-2LR\cos\left(2\delta-\frac{\pi}{2}\right)}{1+L^2R^2-2LR\cos\left(2\delta-\frac{\pi}{2}\right)} \tag{2.8}$$

3. SIMULATION AND ANALYSIS

In accordance with the previous study, the intensity loss in the resonant cavity was influenced by the optical elements and it must to be evaluated. In Fig 2, the intensity loss of the optical elements is measured by the optical power meter at each blue position. In the experiment, the measured intensity loss in the resonant cavity is about 86%.

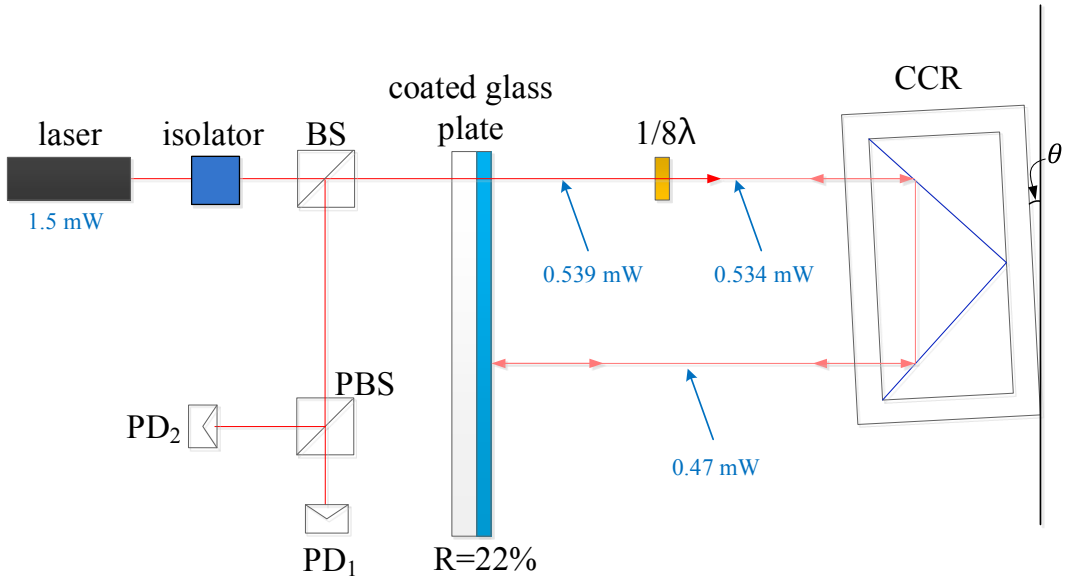

Fig. 2 Intensity loss in the resonant cavity

The intensity loss in the resonant cavity and the reflectance of 20% and 90% are substituted into the equation 2.7 and 2.8. The corresponding interferometric intensity distributions are demonstrated in Figure 3 and 4.

The simulation results reveal that the reflectance of the planar mirror will affect the energy utilization, the fineness of the interferometric signals, the magnitude and the proximity of the amplitude in the each quadrant. Hence the boundary conditions of the optimized reflectance are necessary to be defined.

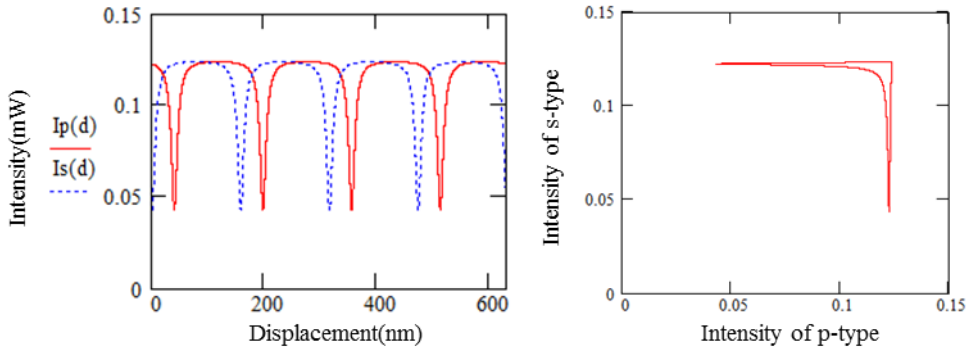

(a) Displacement vs. Intensity (b) s-p type

Fig. 3 Signal distribution by simulation (R: 90%)

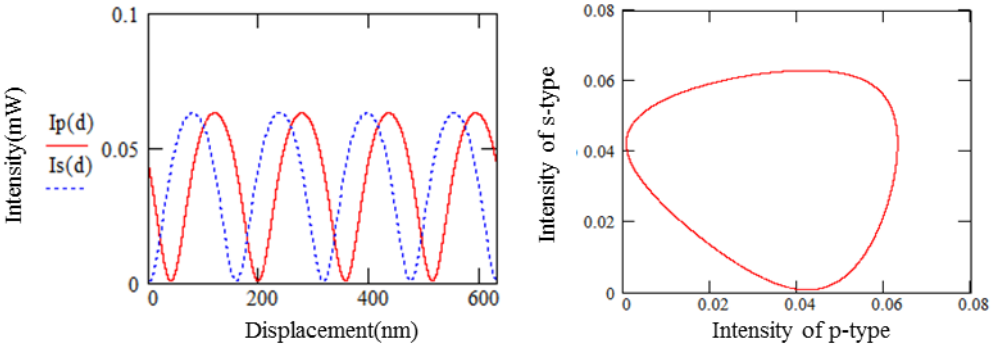

(a) Displacement vs. Intensity (b) s-p type

Fig. 4 Signal distribution by simulation (R: 20%)

To achieve the signal processing function of fine division in the four quadrants, the resolution of each quadrant must be close. Two boundary conditions for defining the reflectance are proposed in this study. The first definition is the amplitude of each quadrant having to be greater than an estimated value. The second definition is the amplitude of each quadrant having to be closer to each other. The Lissajous figure are divided into four quadrants by the maximum signal value of x-axis and y-axis, that is, the peaks of the interferometric signal are as endpoints. Therefore, the period of the interferometric signal can be divided into four equal parts. Because 1st and 3rd quadrant are symmetrical to the straight line with the equation x = y, the amplitude in 1st quadrant and in 3rd quadrant are defined as a and b. The sketch of the light intensity distribution of four quadrants has been illustrated in Fig. 5.

©2017 - TU Ilmenau

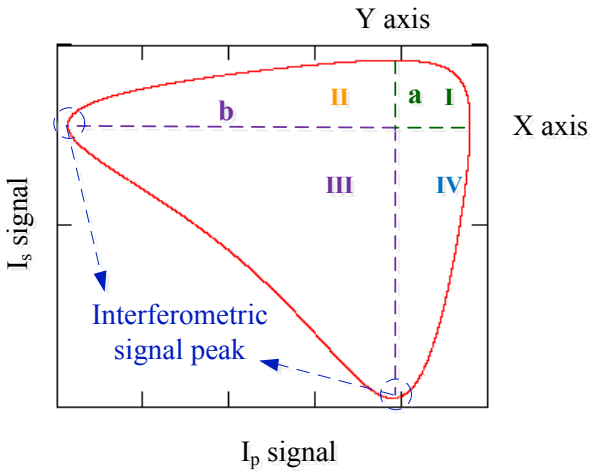

Fig. 5 Division of four quadrants

Each reflectance is substituted into equation 2.7 and 2.8, and then the amplitude from two endpoints to the center of the each Lissajous figure can be obtained. From the simulated results, the amplitude in 1st quadrant is smaller than the other quadrants. Therefore, the maximum value of the amplitude in 1st quadrant is selected for the judgement of the optimized amplitude. Based on the following simulated results, the maximum amplitude in 1st quadrant can be obtained as shown in Table 1. The interferometric intensity distributions are illustrated in Figure 6.

Table 1 Corresponding amplitude in 1st quadrant

1st Quadrant / Reflectance (%)	Amplitude
23	0.021195
24	0.021256
25	0.021275
26	0.021253
27	0.021194

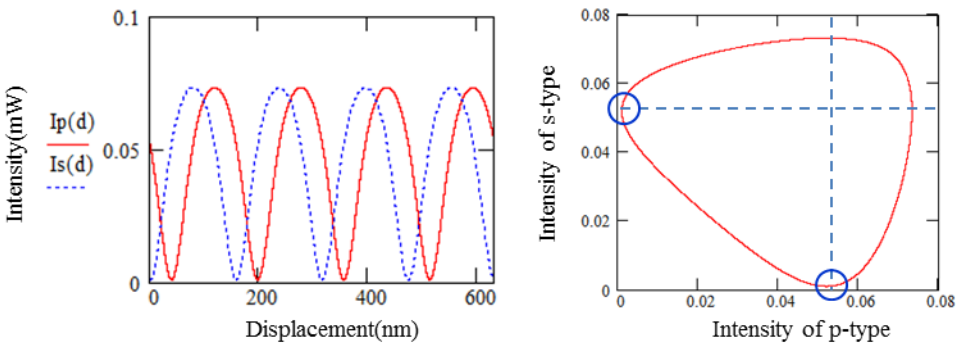

(a) Displacement vs. Intensity (b) s-p type

Fig. 6 Signal distribution by simulation (R: 25%)

However, the uniformity of the amplitude in each quadrant (R: 25%) is not applicable and the reflectance is inversely proportional to the uniformity of the amplitude, the range of the selected reflectance must be redefined between 1% and 25%. The method of the selected reflectance is as the following description, and the definition of the related parameters are demonstrated in Table 2 and Table 4.

To represent the degree of the amplitude decline, the differences between the amplitude of the corresponding reflectance (R_n) and the corresponding maximum reflectance ($R_{n'}$) in 1st quadrant are divided by the amplitude of the corresponding maximum reflectance as shown in equation 3.1. And the change rate in amplitude decline can be obtained by the equation 3.2. The simulated results are listed in Table 3.

$$A_d = (A_{Rn'} - A_{Rn})/A_{Rn'} \tag{3.1}$$

$$r_d = A_{d+1} - A_d \tag{3.2}$$

Table 2 Related parameters of the amplitude decline

Symbol Table	
R_n	Reflectance (n: 1 ~ 24%)
$R_{n'}$	Reflectance (n′: 25%)
A_{Rn}	Amplitude (R: 1 ~ 24 %)
$A_{Rn'}$	Maximum amplitude (R: 25 %)
A_d	Amplitude decline
r_d	The rate of change in amplitude decline

Table 3 Simulated results of the amplitude decline

R_n	A_{Rn}	A_d (%)	r_d (%)
1	0.002076	90.2	9.0
2	0.004011	81.2	8.5
3	0.005809	72.7	7.8
≈	≈	≈	≈
22	0.021088	0.9	0.5
23	0.021195	0.4	0.3
24	0.021256	0.1	0.1
$R_{n'}$	$A_{Rn'}$		
25	0.021275		

To represent the degree of the amplitude proximity, the differences between the maximum amplitude and the minimum amplitude of each corresponding reflectance are divided by the difference between the maximum amplitude and the minimum amplitude of the corresponding maximum reflectance as demonstrated in equation 3.3. The change rate in amplitude proximity can be obtained by the equation 3.4. The simulated results are listed in Table 5.

$$A_p = |b_{Rn} - a_{Rn}| \ / \ |b_{Rn'} - a_{Rn'}| \tag{3.3}$$

$$r_p = A_{p+1} - A_p \tag{3.4}$$

Table 4 Related parameters of the amplitude proximity

Symbol Table	
R_n	Reflectance (n: 1 ~ 24%)
$R_{n'}$	Reflectance (n: 25%)
a	Amplitude of 1st quadrant
b	Amplitude of 3rd quadrant
A_p	Amplitude proximity
r_p	The rate of change in amplitude proximity

Table 5 Simulated results of the amplitude proximity

R_n (%)	$b_{Rn} - a_{Rn}$	A_p (%)	r_p (%)
1	0.000072	0.2	0.8
2	0.000285	1	1.0
3	0.000631	2	1.6
≈	≈	≈	≈
22	0.024277	81.8	6.0
23	0.026059	87.8	6.1
24	0.027865	93.9	6.2
$R_{n'}$	$b_{Rn'} - a_{Rn'}$		
25	0.029691		

From the results of r_d and r_p, the two change rates are inversely proportional to each other with the change of the reflectance. In order to determine the cross/optimal point between two change rates, the curves of these two rates are demonstrated in Fig. 7. The obtained intersection point (R: 12%) is the optimal value of the reflectance as shown in Fig. 8.

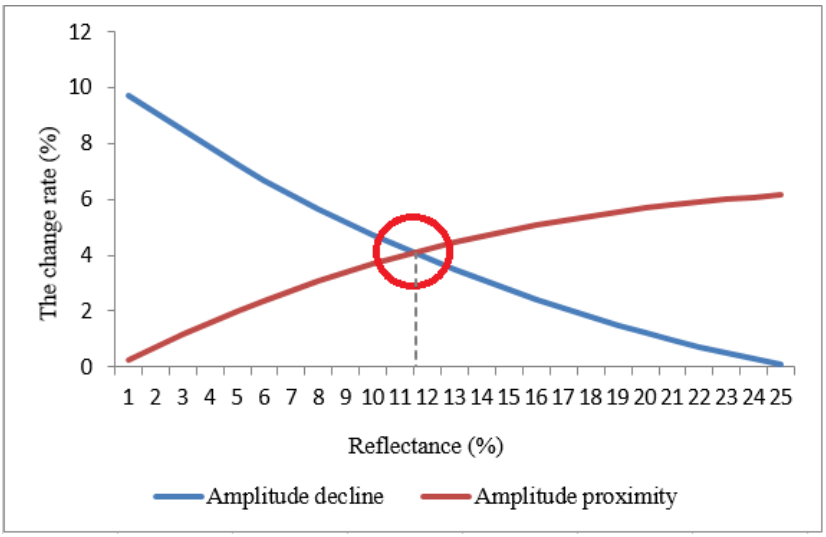

Fig. 7 Curves of two rates

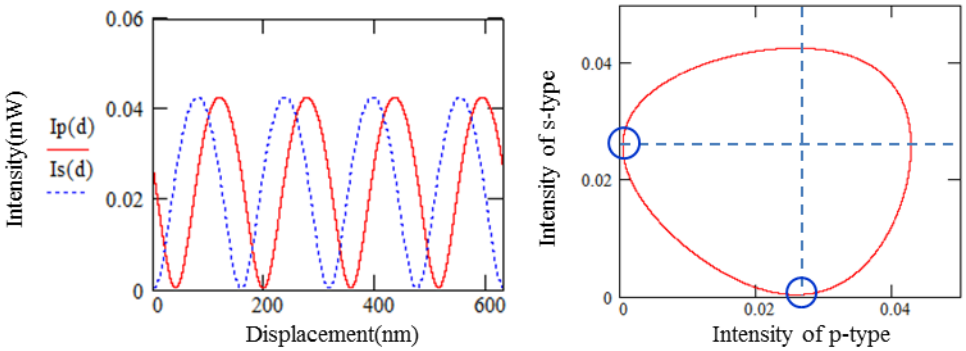

(a) Displacement vs. Intensity (b) s-p type

Fig. 8 Signal distribution by simulation (R: 12%)

4. CONCLUSION

The fineness of the interferometric signal is influenced by the intensity loss of the resonant cavity and the reflectance of the planar mirror. By considering the reflectance of the planar mirror and the intensity loss of the resonant cavity to construct the theoretical simulation in this paper is realized. The experimental results reveal that the intensity loss in the resonant cavity is 86%. And by the simulated results, the optimized reflectance of the planar mirror is 12%.

REFERENCES

[1] P. Rabinowitz, S. F. Jacobs, T. Shultz, and G. Gould, "Cube-corner Fabry-Perot interferometer," Journal of the Optical Society of America, Vol. 52, pp. 452-453, 1961.

[2] Edson R. Peck, "Polarization properties of corner reflectors and cavities," Journal of the Optical Society of America, vol. 52, pp. 253-257, 1961.

[3] James L. Zurasky, "Cube corner retroreflector test and analysis," Applied Optics, Vol. 15, pp. 445-452, 1976.

[4] Jian Liu, and R. M. A. Azzam, "Polarization properties of corner-cube retroreflectors: Theory and Experiment," Applied Optics, Vol. 36, pp. 1553-1559, 1997.

[5] Ki-Nam Joo, Jonathan D Ellis, Jo W Spronck and Robert H Munnig Schmidt, “Design of a folded, multi-pass Fabry-Perot cavity for displacement metrology”, Meas. Sci. Tech., Vol. 20, pp. 107001(5pp), 2009.
[6] C. P. Chang, L. H. Shyu, P. C. Tung, and Y. C. Wang, “Multibeam interferometer for displacement measurements in the large measuring range,” in Proceedings of the 2nd International Conference on Nano-manufacturing, Tianjin, China, 24–26 September, 2010.

CONTACTS

Yung-Cheng Wang wangyc@yuntech.edu.tw
Lih-Horng Shyu lhshyu@nfu.edu.tw
Hung-Ta Shih citizen201322@gmail.com